Fish and Shellfish Immunology 146 (2024) 109398

Contents lists available at ScienceDirect

Fish and Shellfish Immunology

journal homepage: www.elsevier.com/locate/fsi

Full length article

Mucous cell histopathology and label-free quantitative proteomic analysis of skin mucus in fat greenling (*Hexagrammos otakii*) infected with *Vibrio harveyi*

Xiaoyan Wei, Yanyan Shi, Shuai Wang, Hui Liu, Zheng Zhang, Lina Yu, Wenyuan Hua, Dandan Cui, Yan Chen, Xuejie Li *, Wei Wang **

Key Laboratory of Applied Biology and Aquaculture of Northern Fishes in Liaoning Province, Dalian Ocean University, Dalian, 116023, China

ARTICLE INFO

Keywords:
Skin
Mucus
Label-free
Hexagrammos otakii
Vibrio harveyi

ABSTRACT

Hexagrammos otakii is favored by consumers and aquaculture practitioners because of its strong adaptability and fast growth. However, recently, frequent outbreaks of diseases in the breeding of *H. otakii* have led to significant economic losses, especially due to bacterial diseases, which limit the healthy breeding of *H. otakii*. As a luminescent Gram-negative bacterium, *Vibrio harveyi* is the main pathogenic bacteria of *H. otakii*. In this study, the histopathology and label-free quantitative proteomics analysis were performed to reveal the changes of skin mucus proteins in *H. otakii* after infection with *V. harveyi*. The histopathological changes in the skin of *H. otakii* showed that when the bacteria were injected into the epithelial cells, it caused an increase in the number of mucous cells and a certain degree of damage and deformation in skin. Moreover, the quantitative proteomics analysis revealed a total of 364 differentially expressed proteins (DEPs), and these DEPs were found to be involved in environmental information processing, metabolism, infectious diseases: bacteria, replication and repair. More importantly, the enrichment analysis of the DEPs revealed that these different proteins were mainly targeted immune-related pathways. After infection of bacteria, the host's immune ability will be weakened, causing *V. harveyi* to enter the organism more easily, resulting in increased mucus in *H. otakii*, which will eventually lead to a decline in its physical function. These results provided an insight into a series of physiological changes after the bacterial infection of fish at the proteomic level and basic data for further exploration of the potential mechanism of skin mucus. Taken together, the results indicated more opportunities for the future designs and discoveries of effective antibacterial vaccines and antibacterial drugs for *H. otakii*.

1. Introduction

Fat greenling (*Hexagrammos otakii*) is a vital commercial fish in the Northwestern Pacific, it is primarily found in China's Bohai Sea, East Sea and Yellow China Sea [1–3]. In recent years, the farming of *Hexagrammos otakii* (*H. otakii*) has suffered significant financial losses due to recurrent disease outbreaks, particularly bacterial illnesses which has limited the growth of a healthy *H. otakii* aquaculture [4]. Vibrio spp., which are rod-shaped bacteria and belong to the gram-negative category, exist naturally and can be observed in various aquatic environments such as freshwater, estuarine, and marine habitats [5]. Vibrio is a large and diverse bacterial group of marine and estuarine environments successfully isolated and identified [6]. *Vibrio harveyi*, *Vibrio eel*, *Vibrio furnissii*, *Vibrio parahaemolyticus*, *Vibrio vulnificus,* and *Vibrio alginolyticus* have been isolated, causing huge economic losses worldwide [7]. In recent years, *H. otakii* has also been affected by Vibrio infections, resulting in reduced production in China [3]. Nevertheless, the disease and immunity aspect of *H. otakii* continues to be overlooked.

Vibrio harveyi (*V. harveyi*) is a luminescent gram-negative bacterium and a dangerous pathogen in natural aquatic ecosystems [3,8]. It is a major cause of vibriosis, one of the deadliest infectious diseases of farmed fish [9]. *V. harveyi* can attach to biological or non-biological surfaces, to a free state of life, or a symbiotic or host-pathogen interaction with other organisms, which is extremely common in both aquatic vertebrates and invertebrates [10], and has caused outbreaks of major diseases in aquaculture, resulting in infected biological diseases and

* Corresponding author.
** Corresponding author.
E-mail addresses: lixuejie@dlou.edu.cn (X. Li), wangwei@dlou.edu.cn (W. Wang).

https://doi.org/10.1016/j.fsi.2024.109398
Received 13 December 2023; Received in revised form 16 January 2024; Accepted 18 January 2024
Available online 18 January 2024

even death [11]. Many pelagic animals were previously known to be infected with *V. harveyi*, including flounder (*Paralichthys olivaceus*), common snakefish (*Centropomus undeeimalis*), and Atlantic salmon (*Salmo salar*) [12–14]. Symptoms of *V. harveyi* infection include eye lesions, slow movement, feeding cessation, gastrointestinal diseases, varying degrees of ulceration on the body surface, and in severe cases, death [15]. However, research on the skin pathogenic mechanism of *V. harveyi* is limited, and the corresponding pathogenic mechanism has not yet been fully elucidated and requires additional investigation.

Fish skin mucus is the first line of defense against the infection of external pathogens [16] and plays a crucial role in controlling the fish's immune system [17]. Three mucus-secreting cells, known as goblet cells, sacciform cells, and club cells, are responsible for its production in the fish skin, with goblet cells producing the majority of fish mucus [18], and being scattered throughout the mucosal tissue with epithelial cells [19,20]. The proteomic analysis of mucus is an easy-to-obtain technique that does not require the sacrifice of animals and only a simple procedure to obtain representative protein contents and to detect the fish immune status [21]. In recent years, under viral and bacterial infections, the skin mucus proteomes of a series of fish species, in particular atlantic cod (*Gadus morhua*), *Boleophthalmus pectinirostris*, crucian carp (*Carassius auratus gibelio*), yellow catfish (*Pelteobagrus fulvidraco*), greater amberjack (*Seriola dumerili*), *Cynoglossus semilaevis*, rainbow trout (*Oncorhynchus mykiss*) and *Anguilla anguilla* [22–29]. At present, the research on the immunity of *H. otakii* remains limited. Therefore, this paper expounds the mucosal immunity of *H. otakii* from the perspective of proteomics.

In this research, we studied the microstructure of the skin tissue by histopathological technique, and we also utilized label-free quantitative mass spectrometry, a proteomics technology, to identify the proteome map of the skin mucus in *H. otakii* during varying concentrations of *V. harveyi* infection, and analyzed the changes of protein content. These studies provide fundamental information on the physiological and pathological changes of *H. otakii* after infection with *V. harveyi*.

2. Materials and methods

2.1. Experimental fish

Healthy *H. otakii* were obtained from Dalian Haolin Aquatic Products Co., Ltd (Dalian, China) and cultured at the Key Laboratory of Applied Biology and Aquaculture (Dalian, China). Before the experiment, a total of 100 healthy *H. otakii* (55.0 ± 5.0 g; 15.0 ± 0.5 cm) were placed in an approximately 1000 L tank with water temperature of (14 ± 1) °C for 1 week, and then fasted for 1 week. The diet was formulated with 40 % fish meal and 30 % soybean meal as the main protein source, 16 % casein and 5 % fish oil as the main fat source. The feed was fed according to 2 % of the body weight of the fish, twice a day (9: 00 and 16: 00) [30]. During the experiment, three biological replicates were conducted at each time point (n = 3). *H. otakii* were randomly divided into three groups, which contained low infection group (LIG), high infection group (HIG) and control group (CG), with three tanks (100 L) equipped with purification devices in each group, and 10 fish in each tank. In addition, not feeding during the experiment. After the experiment, all *H. otakii* were treated with medicated bath. The experimental process was shown in Fig. 1.

2.2. Bacterial infection

Bacterial infection was performed according to Siddik's method [31]. Briefly, *V. harveyi* was removed from the aquatic animal hospital at Dalian Ocean University. *V. harveyi* stored at −80 °C was thawed and activated on 2216E agar at 28 °C for 24 h. Subsequently, a single colony was inoculated into 2216E broth and shaken at 28 °C (180 rpm) for 24 h.

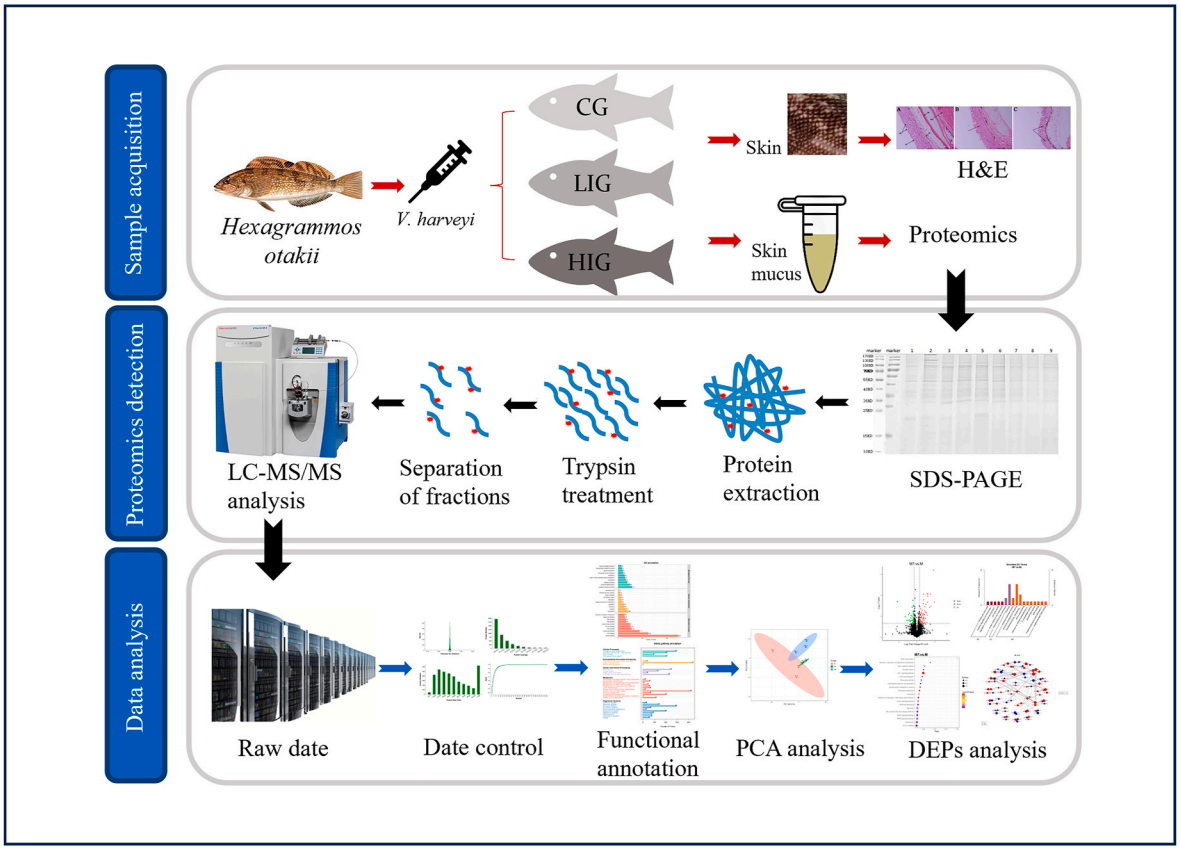

Fig. 1. A schematic illustration of the workflow methodology from sample acquisition to label-free analysis.

The bacterial concentration was determined through the plate counting method, followed by dilution with PBS to the required concentration of 1×10^7 CFU/mL (LIG) and 1×10^8 CFU/mL (HIG), and then 100 μL was injected intraperitoneally into the two experimental groups. Meanwhile, the CG was injected with 100 μL PBS.

2.3. Mucus samples collection

Mucus collection was slightly modified based the method described by Guardiola et al. [32]. After 24 h of injection, *H. otakii* were sedated using 100 mg/L of trichloromethane sulfonate (MS-222, USA) and then rinsed with deionized water, three randomly selected fish from each tank (composite sample) collect mucus from the skin of *H. otakii*. Then, the dorsal surface of *H. otakii* was gently scraped by using a cell scraper, while taking care to avoid contamination with blood, urine and feces. Subsequently, mucus samples were immediately frozen using liquid nitrogen and then stored at −80 °C for subsequent proteomic analysis.

2.4. Histopathological analysis

After the mucus was taken, the dorsal lateral region of the fish's skin was dissected (1 cm^2), rinsed with normal saline, and immediately fixed in 4 % paraformaldehyde for histopathological analysis. The fixed skin samples were removed with 70 % alcohol to remove excess Bouin's solution, and then the tissues were dehydrated with different gradients of ethanol solution, followed by infiltration and paraffin embedding, and finally paraffin blocks were prepared. Neatly, the paraffin sections of 3–4 μm were cut using the Leica RM2125 microtome in a precise manner, following which they were placed on the slide. Lastly, the paraffin sections were stained with hematoxylin-eosin (H & E), and the pathological changes were observed and photographed under the Leica (LEICA DM4000 LED) microscope.

2.5. Total protein extraction and SDS-PAGE

Total protein was extracted through the utilization of the Bradford protein quantification kit (Beyotime Biotechnology). The method was described by Zhang et al. [33]. The mucus was incubated with protein lysates (8 M urea, 100 mM TEAB, pH 8). It was then treated with ultrasound 2 × 5 s (Ningbo Xinzhi/JY92-11 N), centrifuged at 12,000 g at 4 °C for 15 min, and the resulting supernatant was collected in a new 1.5 mL centrifuge tube. The solution was added with 1 M dithiothreitol (DTT) for 1 h at 56 °C, then treated with enough iodoacetamide (IAM) for 1 h at room temperature in darkness, followed by a 2 min ice bath.

After extraction, protein concentration was evaluated through the Bradford method, with bovine serum albumin (BSA) as the standard. The samples were then subjected to 15 % SDS-PAGE gel electrophoresis, heated to boiling, rapidly stained with Coomassie Brilliant Blue (CBB) and observed for decolorization after 15 min (Fig. 1).

2.6. Proteolysis

As described by Zhang H et al. [34]. Protein samples were obtained and the protein solution was supplemented to a volume of 100 μL. Subsequently, 100 mM TEAB buffer and trypsin were added, followed by an incubation period of 4 h at 37 °C. Overnight digestion was achieved by adding trypsin and $CaCl_2$. The pH was reduced to below 3 by introducing formic acid. Following mixing, the mixture was centrifuged for 5 min at 12,000 g and room temperature. The resulting supernatant was passed through the C18 desalination column, continuously washed three times with a cleaning solution (0.1 % formic acid, 3 % acetonitrile). Then, an adequate quantity of eluent containing (0.1 % formic acid, 70 % acetonitrile) was added. The filtrate was collected and freeze-dried afterwards.

2.7. Label-free quantitative proteomics

Liquid chromatography-tandem mass spectrometry (LC-MS/MS) analysis was performed using an EASY-nLC™ 1200 nano-upgrade UHPLC system and a Q Exactive™ HF-X mass spectrometer (Thermo Fisher/LC140) [35]. The mobile phases, A (100 % water, 0.1 % formic acid) and B (80 % acetonitrile, 0.1 % formic acid) were combined and 10 μL of mobile phase A was used to dissolve the lyophilized powder. After centrifuging the mixture at 4 °C and 14,000 g for 20 min, 1 μg of the resulting supernatant was injected into the self-made pre-column (inner diameter 4.5 cm × 75 μm, particle size 3 μm). The mixture was subsequently purified at a flow rate of 5 μL/min for 5 min. In the EASY-Spray chromatographic column (Acclaim Pep Map C18, pore size 96 Å, inner diameter 15 cm × 150 μm, particle size 1.9 μm, Thermo Scientific), the peptides were converted in the phase B solution using a linear gradient (10–30 %) and a flow rate of 250 nL/min for 2 h. All biological replicates were run at an LC gradient of 120 min.

Data-dependent acquisition mode was employed in mass spectrometry. The mass spectrometry full scan range was m/z 350–1500 and the first order resolution was set at 60,000 (200 m/z). The high-energy collision fragmentation (HCD) method was used for fragmentation and secondary mass spectrometry detection. The resolution of the second-order mass spectrometry was set to 15,000 (200 m/z). The dynamic range was set to 20 s, and the mass tolerance was 10 ppm. Ultimately, Finally, the raw data of mass spectrometry were produced.

2.8. Statistical analysis

Western blot analysis are performed as described in Li et al. [36]. After adjusting the concentration of the total protein solution, the sample buffer was boiled. The supernatant was then centrifuged at 12, 000 rpm for 10 min at 4 °C for gel electrophoresis. Proteins were separated by 7.5 %, 10 % and 15 % SDS-PAGE, and the gels were then transferred to a methanol-activated PVDF membrane (Immobilon-P, USA) for 30 s. The primary antibodies used in the experiments were purchased from ProteinTech Group, Inc. (Stathmin 1, 11157-1-AP; RBX1, 14895-1-AP; PSMA6, 11573-1-AP; Beta Actin, 66009-1-IG; ERK1/2, 11257-1-AP; CADM1, 14335-1-AP; Septin 9, 10769-1-AP; NF-κB, 10745-1-AP; Integrin Beta 1, 12594-1-AP and Hexokinase 2, 22029-1-AP) and diluted according to the optimal dilution ratio of different antibodies. Additionally, we used horseradish peroxidase-labelled (HRP-labelled) secondary antibodies, including goat anti-rabbit IgG (H + L, 1:10,000, Biodragon) and goat anti-mouse IgG (H + L, 1:5000, Beyotime). The results were observed using the BeyoECL Plus Kit (Beyotime) on a Western blot imager (Amersham Imager 600, USA).

2.9. Statistical analysis

The resulting spectra were searched according to the genome data of *Anoplopoma fimbria* (BioProject PRJNA 869752) from NCBI using the Proteome Discoverer search engine (Thermo, HFX). The Peptide Spectrum Matches (PSMs) were filtered using Proteome Discoverer (PD) software, ensuring a credibility of over 99 %. Verification of the FDR was conducted to determine the critical threshold, which was set at FDR <0.01. The normality of the evaluation data was tested using the Shapiro-Wilk method, then followed by the use of the T-test for statistical analysis of the protein quantitative results. Differentially expressed proteins (DEPs) were defined as those whose quantitation was significantly different between experimental and control groups ($P < 0.05$ and $|\log2FC| > 0.5$ (FC > 1.5 or FC < 0.67 [fold change, FC])). The analysis of data used the public Gene Ontology (GO) database (http://www.geneontology.org/), the Kyoto Encyclopedia of Genes and Genomes (KEGG) database (http://www.genome.jp/kegg/pathway.html) and the Eukaryotic Orthologous Groups (http://www.ncbi.nlm.nih.gov/KOG).

3. Results

3.1. Changes in the skin of H.otakii after infection with V. harveyi

Fig. S1 illustrated the macroscopic lesions of *H. otakii* during rearing process, caused by *V. harveyi* infection. The outcomes exhibited healthy adult fish (Fig. S1A), fish infected with *V. harveyi* exhibiting cutaneous sores and ulceration (Fig. S1B), and a magnified view of the skin ulceration after *V. harveyi* infection (Fig. S1C). The H&E staining of skin paraffin sections showed three main features. First, compared with the CG group (Fig. 2A), the number of mucous cells in the LIG group (Fig. 2B) and the HIG group (Fig. 2C) increased significantly. Second, stress changed the location and morphology of pigment cells. The pigment clusters in the HIG group were thicker and deeper, while the pigment in the LIG group was lighter. Third, the destruction of the epithelial tight junction layer was observed in both LIG group and the HIG group (Fig. 2B), as well as signs of cell infiltration and inflammatory processes were observed in both groups.

3.2. Identification of skin mucus from H. otakii

The UHPLC-MS/MS analysis revealed a total of 536,661 spectra, 162,442 matched spectra, and 19,870 peptide sequences were obtained. Removal of redundant peptides identified 3787 non-redundant proteins (Table 1). The 48.98 % of reliable proteins had sequence coverage of >10 %, indicating good coverage (Fig. 3A). The identified proteins have a wide range of mass distribution, with a majority of relative molecular mass below 100 kDa, and a small amount greater than 100 kDa (Fig. 3B).

Additional annotation and analysis of the discovered proteins was performed in the GO and KEGG databases (Fig. 4). In the GO classification, 2277 proteins were assigned to 727 terms, which were categorized into three groups: molecular function (MF), cellular component (CC) and biological process (BP). In the BP category, the proteins with an oxidation-reduction process are the most, followed by 'protein phosphorylation' and 'metabolic process'. The CC category significantly expresses the proteins associated with the 'intracellular' and 'nucleus'. In the MF category, the term that appears most frequently is 'protein binding' (Fig. 4A). In the KEGG pathway annotation, 3545 proteins were assigned to 33 categories, of which the most abundant pathway was 'Signaling molecules and interaction', followed by 'Glycan biosynthesis and metabolism' and 'Transport and catabolism' pathways (Fig. 4B). In the KOGs classification, 3453 proteins were assigned to 25 categories, with 36 % of DEPs allocated to posttranslational modification, protein turnover, chaperone, general function prediction only, and signal transduction mechanism (Fig. 4C). The above results indicate that the mucus of *H.otakii* are involved in multiple cellular and biological processes.

3.3. Analysis of DEPs

A total of 163, 211, and 72 DEPs ($P < 0.05$) were identified as significant between groups LIG and CG, HIG and CG, and HIG and LIG, separately. Overall, 101 DEPs were increased and 62 DEPs were decreased in the LIG and CG groups; 108 DEPs were increased in the HIG group and 103 DEPs were decreased in the CG group; compared to the LIG group, 38 DEPs were increased and 34 DEPs were decreased in the HIG group (Fig. 5A). Three sets of DEPs were presented through the comparison of volcano plots (Fig. 5B). The Venn diagram illustrates the intersection of DEPs in the three groups (Fig. 5C). Additional clustering analysis highlighted that these DEPs were primarily clustered into two comparisons: LIG *vs.* CG and group HIG *vs.* CG (Fig. 5D).

Table 1
Summary of Label-free DIA database search analysis.

Name	Total spectra	Matched spectrum	Peptide	Identified protein
All	536,661	162,442	19,870	3787

3.4. Functional enrichment analysis of DEPs

Firstly, we analyzed the function of DEPs through GO enrichment. Fig. 6A showed the abundance of elements ($P < 0.05$) in three distinct groups (MF, CC, and BP). The results demonstrated that the DEPs of LIG and CG were mainly distributed in the CC class's ribosome and mitochondrial outer membrane. BP and DEPs are mainly involved in protein insertion into the membrane, cell cycle arrest, and tricarboxylic acid cycle. MF DEPs mainly involved palmitoyl hydrolase activity, fine transferase activity, and structural constituent of ribosome. The DEPs of HIG and CG were mainly distributed in the intracellular and intracellular parts of the CC class. BP and DEPs are mainly involved in the compound nitrogen metabolic process, cellular compound nitrogen metabolism, and cellular biosynthetic process. The MF-type DEPs mainly involve structural molecule activity and structural constituent of ribosome. The DEPs of HIG and LIG were mainly distributed in the CC class ESCRT I complex. MF DEPs mainly involve hydroxymethylglutaryl-CoA synthase activity, phosphatidylinositol-4-phosphate binding, and syntaxin binding.

In the KEGG pathway enrichment analysis, 177 KEGG pathways were detected in the LIG and CG groups (Fig. 6B). Among them, the Neomycin, kanamycin and gentamicin biosynthesis signaling pathways related to metabolism, the HIF-1 signaling pathway related to signal transduction in Environmental information processing, and the MAPK signaling pathway were significantly enriched. KEGG pathway enrichment analysis in CG and HIG groups identified 109 KEGG pathways; the changes in Steroid Hormone Biosynthesis, Neomycin, Kanamycin and Kanamycin Kiosynthesis, Bacterial invasion of Epithelial Cells were more significant. In the LIG and HIG groups, KEGG pathway enrichment analysis detected 113 KEGG pathways. Moreover, signaling pathways were significantly enriched, including Cell adhesion molecules (CAMs), Nucleotide excision repair, and 2-Oxocarboxylic acid metabolism. The DEPs of these major pathways were listed in Table 2, and 10 DEPs (Stathmin 1, RBX1, PSMA6, Beta Actin, ERK1/2, CADM1, Septin 9, NF-

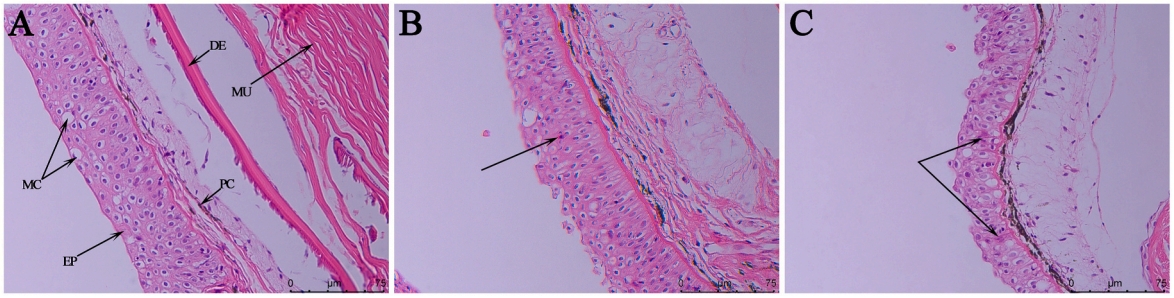

Fig. 2. The histopathological changes of the skin of *H.otakii* infected with low and high concentrations of *V.harveyi* were observed by H & E staining. Epidermal cells (EPs), dermal cells (DEs), muscle (MU), mucous cells (MCs) and pigment clusters (PCs) **(A)**. The arrow indicates inflammatory cell infiltration **(B, C)**. Bar = 75 μm.

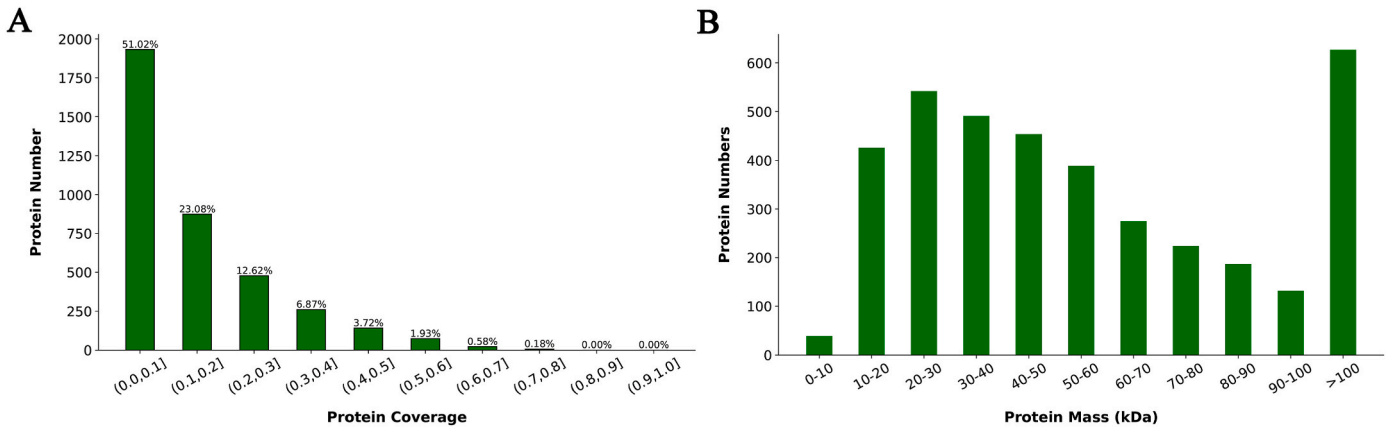

Fig. 3. Protein information map. **(A)** Protein coverage distribution histogram. The abscissa is the interval of protein coverage (the length of the protein covered by the detected peptide segment/the full length of the protein), and the ordinate is the number of proteins contained in the corresponding interval. **(B)** Protein molecular weight distribution. The abscissa is the molecular weight of the identified protein (unit: kDa), and the ordinate is the number of identified proteins.

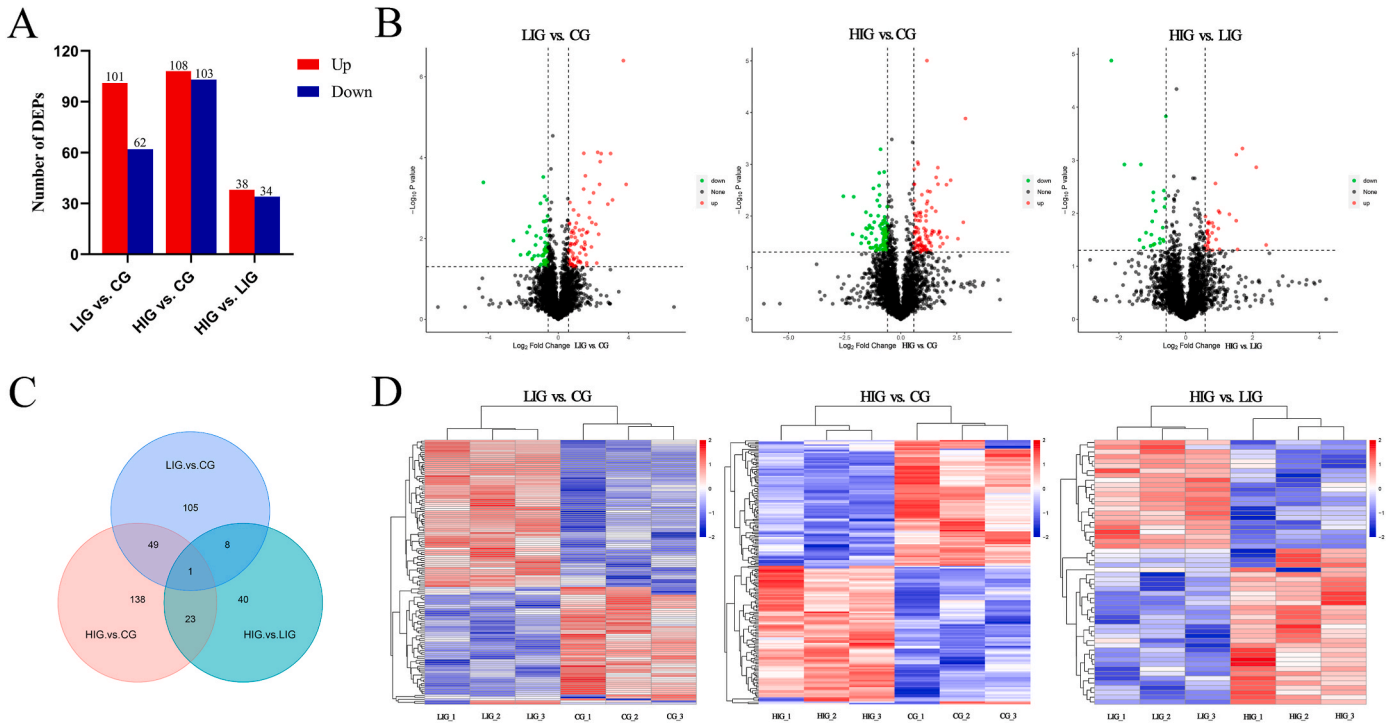

Fig. 4. GO and KEGG annotation analysis of mucus proteins. **(A)** GO annotation. **(B)** KEGG pathway annotation. **(C)** KOG pathway annotation.

κB, Integrin Beta 1 and Hexokinase 2) were randomly selected for verification by Western blot. The results showed that the differential expression trend was consistent with the results of proteomics (Fig. 7).

KOGs enrichment analysis showed that DEPs in skin mucus of *H. otakii* were enriched into 24 functional categories (Fig. 6C–Table S1). Obviously, the three groups of DEPs are mostly concentrated in translation, ribosomal structure and biosynthesis; general function prediction only; post-translational modification, protein turnover, chaperone; signal transduction mechanism and intracellular trafficking, secretion and vesicular transport process. In the LIG *vs.* CG groups and HIG *vs.* LIG groups, DEPs were most expressed in the signal transduction mechanism, while in the HIG *vs.* LIG groups, they were mainly concentrated in translation, ribosomal structure and biosynthesis.

4. Discussion

V.harveyi is the most prevalent pathogenic Vibrio species [8] and is widely distributed in cultured seawater and aquatic animals in vivo and in vitro. However, *H. otakii* is susceptible to Vibrio infection in large-scale aquaculture, resulting in significant economic losses [4]. Therefore, for the safe and efficient breeding of *H. otakii*, it is important to study its immune defense mechanism. The surface mucus of fish plays a significant physiological role in fish growth in the complex aquatic environment [37], and it is also the first line of defense of the fish immune system [24]. Numerous immune components on the surface of fish skin include glycoproteins, complement proteins, C-reactive proteins, lectins, proteolytic enzymes, antimicrobial peptides, flavoenzymes, and immunoglobulins [16,38].

In contrast to mammals, teleost skin exhibits unparalleled histological diversity and uniqueness, and it secretes mucus related to immune

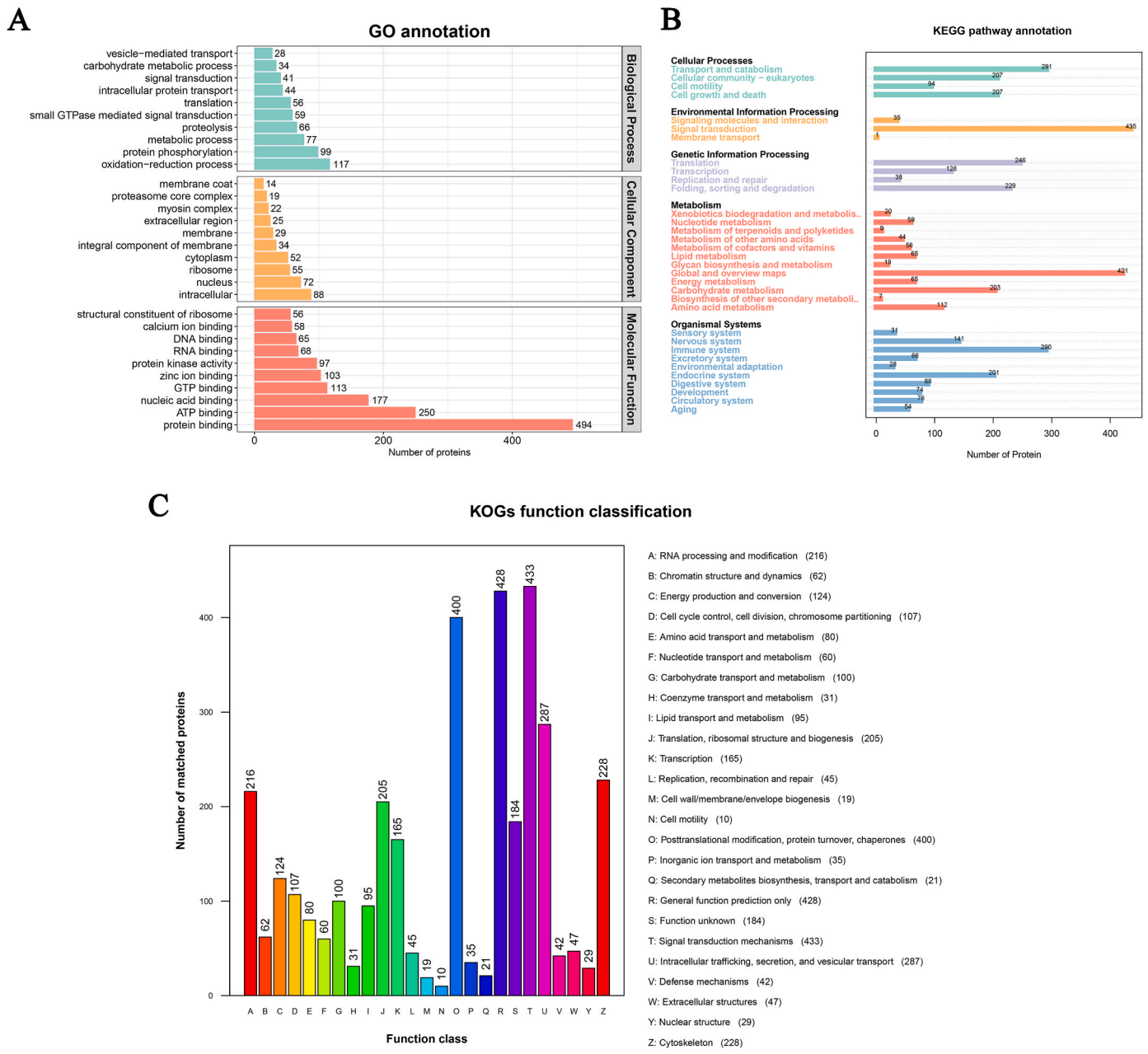

Fig. 5. Differentially expressed proteins. **(A)** Number of DEGs. **(B)** Volcano plot in the three comparisons (Blue and red dots indicate DEGs (FDR <0.05), black dots indicate non-differentially expressed proteins). **(C)** Venn diagram reflected the crossover of DEGs. **(D)** Hierarchical clustering analysis of DEGs (Blue, red and white indicate decrease, increase and no detectable changes in the expression abundance of DEGs, respectively).

function, particularly when stimulated [39]. As the Vibrio concentration increased, the number of mucous cells in the skin increased gradually, and new cells differentiated and moved to the surface of the epidermis (Fig. 2). In response to external stimuli, the fish secretes more mucus. Most studies have reported that goblet cell proliferation or hypertrophy indicates increased mucus production in response to multiple environmental stressors [40,41]. Changes in melanin concentration and melanosome fluidity in fish skin can be observed in reply to external stimuli [42]. Additionally, the study of *Oncorhynchus mykiss* [43] and *Salmo salar* [44] indicated a direct relationship between the color morphology of melanin and stress response and health status. Our results of increased skin pigment clusters align with the reported studies. Epithelial cells of the skin's outer layer exhibit a certain level of destruction and degeneration, even leading to the shedding of necrotic cells. Relevant studies have reported that the pathological changes of acute toxicity on the epidermis of *Heteropneustes fossilis* [45] show that when the external environment stimulates the epithelial cells, they will cause cell shedding and cause a certain degree of damage and deformation [42], as shown in Fig. 2B and C [45].

Proteomics analysis was used to analyze the skin mucus of *H. otakii* infected with *V. harveyi*. The protein distribution histogram, together with the protein molecular weight distribution map, showed that the protein molecular weight distribution determined by this proteomics was uniform and wide, and the quality was qualified (Fig. 3). The skin mucus of *H. otakii* has a potential to exhibit diverse and complex functions, as evidenced by the mapping of the 3787 proteins identified through proteomics analysis to 727 items of GO classification and 33 items of KEGG pathway annotation (Fig. 4). Additionally, by analyzing the changes of mucus before and after *V. harveyi* infection in *H. otakii*, some changes in key proteins were found (Table 2). GO, KEGG and KOG

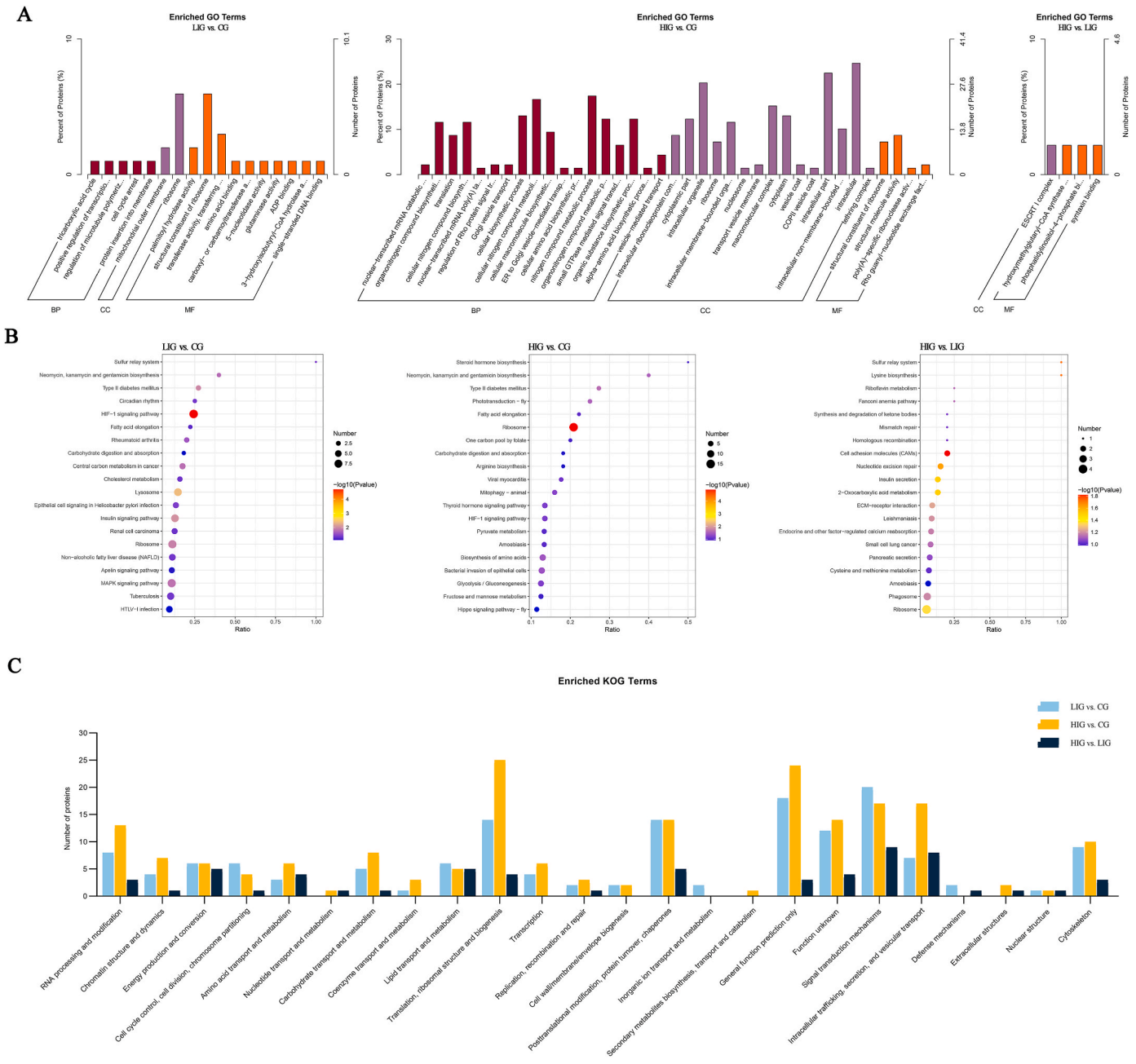

Fig. 6. Functional analysis of significantly enriched trends. **(A)** GO Enriched Terms of Meaning for Molecular Functions (MF), Cellular Components (CC) and Biological Processes (BP). **(B)** The top 20 significance terms of KEGG enrichment. **(C)** KOG enrichment for 24 functional categories.

enrichment analysis of these proteins evidenced that the differential proteins mainly involved Environmental Information Processing, Metabolism, Infectious disease: bacterial, Replication and repair (Fig. 5). Most of the major pathway's key proteins are associated with mucosal immunity. This indicates that mucus plays an important defensive role in resisting bacterial invasion, which is consistent with the previous results [25,28].

HIF-1 signaling pathway and MAPK signaling pathway were significantly enriched in LIG and CG groups (Fig. 6B). Hypoxia-inducible factor 1 (HIF-1) is a transcription factor with a basic helix-loop-helix-PAS domain [46]. HIF-1 signaling pathway serves various biological purposes as a classic body response to hypoxia concentration or hypoxia response pathway [47]. The expression of NF-κB protein (Table 2) is significantly increased, which will upregulate HIF-α in this pathway, and HIF-α will promote the expression of cytokines [48]. Cytokines can stimulate the recruitment and activation of bone marrow-derived suppressor cells (MDSC), regulatory T cells (Treg) and tumor-associated macrophages (TAM) [49], thereby inhibiting the adaptive immune system and eventually creating an immunosuppressive environment. Therefore, we hypothesize that when *V. harveyi* invades *H. otakii*, the immune system function in *H. otakii* can be weakened by stimulating the expression of NF-κB. This is consistent with the results of *V. parahaemolyticus* stimulating *Penaeus vannamei* [50] to activate the NF-κB pathway and negatively regulate the immune response to bacterial infection. Nuclear factor of activated T-cells, cytoplasmic 2-like (NFATC) is an important transcription factor, which is closely related to many pathological processes such as cell differentiation, proliferation and apoptosis, and its expression is regulated by MAPK signaling pathway. MAPK signaling pathway is a process of cascade phosphorylation, which can be divided into four classical MAPK pathways: ERK,

Table 2
DEPs in important immune-related KEGG pathways in LIG *vs.* CG, HIG *vs.* CG and HIG *vs.* LIG groups.

Groups	Prot ID	Name	KEGG Description (AD)	P-value	log_2FC[a]
LIG *vs.* CG	AfiChr100828.1	histone acetyltransferase KAT6A [*Seriola lalandi dorsalis*]	Hexokinase (HK)	0.0407	2.1846
	AfiChr080434.1	Hypothetical protein D9C73_002278 [*Collichthys lucidus*]	small subunit ribosomal protein S6e(rpS6)	0.0229	1.2135
	AfiChr070236.1	alkaline phosphatase, tissue-nonspecific isozyme [*Seriola dumerili*]	translation initiation factor 4G (ALPL)	0.0078	2.2941
	AfiChr040431.1	hypothetical protein E3U43_007611, partial [*Larimichthys crocea*]	calcium/calmodulin-dependent protein kinase (CaM kinase) II(Camk)	0.0190	0.6041
	AfiChr230223.1	peroxisome proliferator-activated receptor alpha 2 [*Lateolabrax japonicus*]	cyclin-dependent kinase inhibitor 1B(p21/p27)	0.0472	0.8474
	AfiChr030022.1	E3 ubiquitin-protein ligase RBX1 [*Danio rerio*]	RING-box protein 1(Rbx1)	0.0005	3.8641
	AfiChr101014.1	G-protein coupled receptor 74 [*Collichthys lucidus*]	mitogen-activated protein kinase 1/3(ERK)	0.0133	0.6767
	AfiChr040318.1	P65 transcription factor, partial [*Siniperca chuatsi*]	transcription factor p65(NF-κB)	0.0202	0.7103
	AfiChr110701.1	PREDICTED: neurogenic locus Notch protein-like isoform X2 [*Cyprinodon variegatus*]	MAP kinase interacting serine/threonine kinase (MNK)	0.0000	-Inf
	AfiChr050445.1	myeloid leukemia factor 2 [*Perca flavescens*]	cell division control protein 42(Cdc42)	0.01781	0.6165
	AfiChr190315.1	PREDICTED: misshapen-like kinase 1 isoform X9 [*Paralichthys olivaceus*]	mitogen-activated protein kinase kinase kinase kinase 4(HGK)	0.0000	Inf
	AfiChr100965.1	kinase suppressor of Ras 2 [*Perca flavescens*]	thousand and one amino acid protein kinase (TAO)	0.0433	−0.7099
	AfiChr200641.1	PREDICTED: serine incorporator 2-like [*Stegastes partitus*]	Stathmin (STMN1)	0.0083	−0.6366
HIG *vs.* CG	AfiChr190756.1	PREDICTED: phosphoglycerate kinase 1 [*Stegastes partitus*]	hexokinase (PGK 1)	0.0188	−0.7487
	AfiChr190058.1	clathrin heavy chain 1 isoform X2 [*Scleropages formosus*]	clathrin heavy chain (Clathrin)	0.0050	−1.0452
	AfiChr030007.1	hypothetical protein CCH79_00013,689 [*Gambusia affinis*]	Beta actin/gamma 1(actin)	0.0015	−0.9555
	AfiChr020841.1	alpha-1,6-mannosyl-glycoprotein 2-beta-N-acetylglucosaminyltransferase-like [*Perca flavescens*]	CD2-associated protein (CD2AP)	0.0232	−0.6494
	AfiChr140735.1	zinc finger protein 217 isoform X1 [*Perca flavescens*]	tyrosine-protein kinase Src(Src)	0.0442	−0.7382
	AfiChr200136.1	wiskott-Aldrich syndrome protein family member 2 [*Larimichthys crocea*]	WAS protein family, member 2(WAVE)	0.0224	−0.7341
	AfiChr240369.1	PREDICTED: LOW QUALITY PROTEIN: junctional adhesion molecule B [*Stegastes partitus*]	junctional adhesion molecule B-like isoform X1	0.0495	0.8782
	AfiChr030470.1	1-phosphatidylinositol 4,5-bisphosphate phosphodiesterase delta-3-A-like [*Perca flavescens*]	phosphatidylinositol phospholipase C, delta	0.0446	−0.7938
	AfiChr010237.1	myeloperoxidase [*Epinephelus coioides*]	eosinophil peroxidase	0.0379	−0.6571
	AfiChr180468.1	proteasome subunit alpha type-6 [*Perca flavescens*]	psma6; proteasome subunit alpha type-6 (PSMA 6)	0.0000	Inf
	AfiChr031119.1	uncharacterized protein LOC114570175 [*Perca flavescens*]	septin 3/9/12(Septin)	0.0000	-Inf
HIG *vs.* LIG	AfiChr150072.1	ABC transporter F family member 4-like isoform X1 [*Perca flavescens*]	integrin beta 1(ITGB1)	0.0000	-Inf
	AfiChr190712.1	hypothetical protein E3U43_022,226 [*Larimichthys crocea*]	cell adhesion molecule 1(IGSF4)	0.0244	0.6594
	AfiChr060694.1	PREDICTED: glypican-6-like [*Stegastes partitus*]	cullin 4(Cul4)	0.0253	−1.0280
	AfiChr050352.1	acid sphingomyelinase-like phosphodiesterase 3b [*Perca flavescens*]	replication factor A2(RPA)	0.0000	-Inf
	AfiChr030028.1	aconitate hydratase, mitochondrial-like [*Perca flavescens*]	aconitate hydratase	0.0053	−0.6110
	AfiChr040527.1	PREDICTED: kynurenine/alpha-aminoadipate aminotransferase, mitochondrial [*Lates calcarifer*]	kynurenine/2-aminoadipate aminotransferase	0.0212	0.6620

[a] Log_2FC. threshold = ± Inf.

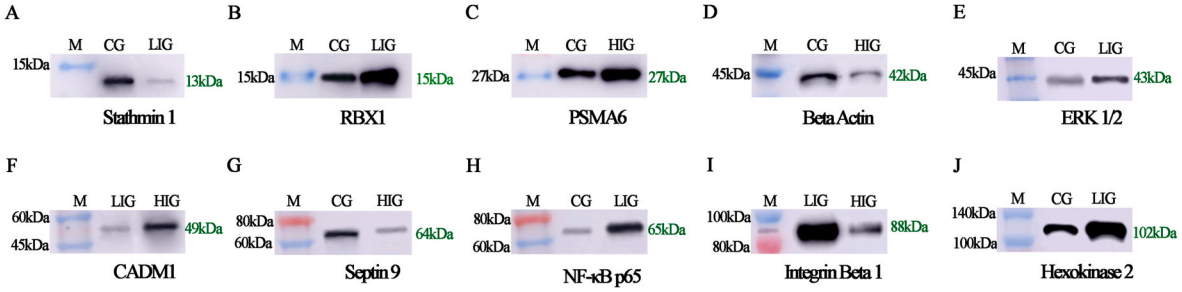

Fig. 7. Verification of DEPs by Western blotting (WB). The WB results for 10 antibodies are presented: **(A)** Stathmin 1, **(B)** RBX1, **(C)** PSMA6, **(D)** Beta Actin, **(E)** ERK1/2, **(F)** CADM1, **(G)** Septin 9, **(H)** NF-κB, **(I)** Integrin Beta 1 and **(J)** Hexokinase 2. Their molecular weights were 13 kDa, 15 kDa, 27 kDa, 42 kDa, 43 kDa, 64 kDa, 65 kDa, 88 kDa and 102 kDa, which were marked in green. Lane M: protein molecular weight marker. Lanes CG, LIG, and HIG were the control group, low injection group, and high injection group, respectively.

p38, JNK, and BMK1, ERK1/2 kinase is the most extensively researched member of the MAPK family [51]. According to proteomics analysis, the expression of ERK protein was significantly increased (Table 2). Some transcription factors may continue to be phosphorylated by ERK1/2, which promotes the expression of genes involved in cell cycle and proliferation [52]. RAKs, MSKs, and MNKs are among the intracellular kinases that activated ERK1/2 can phosphorylate. These kinases affect cell growth and adhesion [51]. In addition, the V-set and transmembrane domain-containing protein 2-like protein (VSTM2L) in the signal transduction mechanisms of the differentially expressed proteins in Fig. 5C and Table S1 was also predicted to enhance the activity of intercellular adhesion mediators and participate in the negative regulation of neuronal apoptosis. This is also consistent with a significant increase in mucus after infection with *V. harveyi* (Fig. 2). Similar results were obtained in the study of *Cynoglossus semilaevis* [53].

Neomycin, kanamycin, and gentamicin biosynthesis were significantly enriched in HIG *vs.* CG and LIG *vs.* CG groups (Fig. 6B). Antibiotics are a class of secondary metabolites produced by microorganisms or

higher organisms during their lifetime with antipathogenic or other bioactive properties. They can act anti-bacterially or bactericidally by hindering the formation of the bacterial cell wall, increasing permeability of the bacterial cell membrane, disrupting the synthesis of bacterial proteins, and inhibiting the replication and transcription of bacterial nucleic acids [54–56]. The hexokinase (HK) expression in this pathway has changed significantly (Table 2). HK has been shown to significantly affect the secretion of mucus but does not affect the bactericidal activity of mucus [16]. The significant enrichment of this pathway indicates that the body of *H. otakii* has recognized the invasion of *V. harveyi* and responded to remove it. In the bacterial invasion of epithelial cells pathway, the expression of Clathrin, CD2AP, Src, WAVE, Septin, and other proteins decreased significantly, decreasing actin protein expression. Actin proteins play a pivotal role in various vital cellular processes such as cell motility, cell division, muscle contraction, cytokinesis, vesicle and organelle movement, cell junction and cell shape establishment, and maintenance [57,58]. Mutations in human actin can lead to muscle disease, heart size and function changes, and deafness [59]. By altering the host's actin skeleton, Gram-negative bacteria infection induces epithelial cells to undergo internalization [60]. When *H. otakii* is infected with *V. harveyi*, another Gram-negative bacterium, the body may undergo similar changes, which is consistent with the results in Fig. 2.

By comparing the KEGG enrichment results of the HIG group and the LIG group, it can be seen that the Cell adhesion molecule, CAMs signaling pathway is significantly enriched, and the expression of the immunoglobulin superfamily IGSF has changed significantly (Table 2). Previous studies have shown that IGSF will initiate complex intracellular molecular interactions after binding to the receptor, ultimately changing the cell gene transcription [61]. Therefore, we predict that *V. harveyi* can affect the transcription of host cells by affecting the expression of IGSF after entering *H. otakii*. This is similar to the immune analysis results of juvenile seabass (*Lates calcarifer*) to *V. harveyi* [62]. Furthermore, our data indicates that the DEPs consist of peroxidase as a crucial antifungal agent and proteases (proteasome subunit alpha type-6: PSAT 6) linked to the immune system's resistance to bacterial or parasitic infections (Table 2). This verifies the significant role of mucus during the immune process.

5. Conclusion

This study focused on the function of protein in skin mucus of *H. otakii* after infected by *V. harveyi*. The histopathological changes of the skin showed that acute stimulation led to an increase in the number of mucous cells, resulting in an increase in mucus secretion and a certain degree of damage and deformation of epithelial tissue cells. In addition, the label-free quantitative proteomics analysis of skin mucus showed that the mucus had the potential to produce complex and diverse functional proteins. From different perspectives, the significant enrichment of HIF-1 signaling pathway, MAPK signaling pathway, neomycin, kanamycin and gentamicin biosynthesis, cell adhesion molecules and CAMs signaling pathway shows that the stimulation of bacteria will lead to immunocompromised, thus affecting the mutual recognition of immune cells, destroying the immune structure of the body, and ultimately causing their body function to decline. Taken together, these results provide basic data for evaluating the potential mechanism of skin mucus in response to *V. harveyi*.

Ethics statement

The care and treatment of the laboratory animals in this investigation were founded on the principles of animal welfare, animal experimentation, and ethical management, and were approved by the Statute of the Experimental Animal Ethics Committee of Dalian Ocean University (No. 2023-51). All subjects participating in the study gave informed consent.

Funding

This work was supported by Applied Basic Research Program of Liaoning Province (2022JH2/101300139), Basic Scientific Research Program of Educational Department of Liaoning Province (JYTZD2023038) and Scientific Research Foundation of Educational Department of Liaoning Province (JL202003).

CRediT authorship contribution statement

Xiaoyan Wei: Investigation, Formal analysis, Data curation, Writing - original draft, wrote the manuscript; Yanyan Shi: Validation, Visualization, Microbiology analysis; Shuai Wang, Hui Liu and Lina Yu: Carried out experiments; Zheng Zhang: Data analysis; Xuejie Li: Methodology, Funding acquisition, Project administration. Writing - review & editing; Wei Wang: Supervision, Funding acquisition.

Declaration of competing interest

The authors declare that they have no known competing financial interests.

Data availability

Data will be made available on request.

Acknowledgements

Thanks to the Key Laboratory of Fish Applied Biology and Aquaculture (Dalian, China) for supporting this study. We also acknowledge the support of *V.harveyi* strain provided by Dalian Ocean University Aquatic Animal Hospital and the proteomics experiment was completed in Novogene Co., Ltd. (Beijing, China). In addition, we would like to express our gratitude to the editorial team at Home for Researchers (www.home-for-researchers.com) for their language editing services.

Appendix A. Supplementary data

Supplementary data to this article can be found online at https://doi.org/10.1016/j.fsi.2024.109398.

References

[1] K.A. Habib, D. Jeong, J.G. Myoung, M.S. Kim, Y.S. Jang, J.S. Shim, Y.H. Lee, Population genetic structure and demographic history of the fat greenling *Hexagrammos otakii*, Genes & Genomics 33 (2011) 413–423.
[2] F. Hu, L. Pan, F. Gao, Y. Jian, X. Wang, L. Li, S. Zhang, W. Guo, Effect of temperature on incubation period and hatching success of fat greenling (*Hexagrammos otakii* Jordan & Starks) eggs, Aquacult. Res. 48 (1) (2017) 361–365.
[3] J. Diao, H. Liu, F. Hu, L. Li, X. Wang, C. Gai, X. Yu, Y. Fan, L. Xu, H. Ye, Transcriptome analysis of immune response in fat greenling (*Hexagrammos otakii*) against *Vibrio harveyi* infection, Fish Shellfish Immunol. 84 (2019) 937–947.
[4] J. Diao, X. Yu, X. Wang, Y. Fan, S. Wang, L. Li, Y. Wang, L. Xu, C. Gai, H. Ye, Full-length transcriptome sequencing combined with RNA-seq analysis revealed the immune response of fat greenling (*Hexagrammos otakii*) to *Vibrio harveyi* in early infection, Microb. Pathog. 149 (2020) 104527.
[5] C. Baker-Austin, J.D. Oliver, M. Alam, A. Ali, M.K. Waldor, F. Qadri, J. Martinez-Urtaza, Vibrio spp. infections, Nat. Rev. Dis. Prim. 4 (1) (2018) 1–19.
[6] P. Heenatigala, Z. Sun, J. Yang, X. Zhao, H. Hou, Expression of LamB vaccine antigen in Wolffia globosa (duck weed) against fish vibriosis, Front. Immunol. 11 (2020) 1857.
[7] H. Dong, S. Taengphu, P. Sangsuriya, W. Charoensapsri, K. Phiwsaiya, T. Sornwatana, P. Khunrae, T. Rattanarojpong, S. Senapin, Recovery of *Vibrio harveyi* from scale drop and muscle necrosis disease in farmed barramundi, Lates calcarifer in Vietnam, Aquaculture 473 (2017) 89–96.
[8] C. Allen, S.E. Finkel, *Vibrio harveyi* exhibits the growth advantage in stationary phase phenotype during long-term incubation, Microbiol. Spectr. 10 (1) (2022) e02144-21.
[9] R. Salini, S. Santhakumari, A.V. Ravi, S.K. Pandian, Synergistic antibiofilm efficacy of undecanoic acid and auxins against quorum sensing mediated biofilm formation of luminescent *Vibrio harveyi*, Aquaculture 498 (2019) 162–170.
[10] I. Montánchez, E. Ogayar, A.H. Plágaro, A. Esteve-Codina, J. Gómez-Garrido, M. Orruño, I. Arana, V.R. Kaberdin, Analysis of *Vibrio harveyi* adaptation in sea

water microcosms at elevated temperature provides insights into the putative mechanisms of its persistence and spread in the time of global warming, Sci. Rep. 9 (1) (2019) 289.
[11] H.T. Nguyen, T.T.T. Nguyen, Y.T. Wang, P.C. Wang, S.C. Chen, Effectiveness of formalin-killed vaccines containing CpG oligodeoxynucleotide 1668 adjuvants against *Vibrio harveyi* in orange-spotted grouper, Fish Shellfish Immunol. 68 (2017) 124–131.
[12] K.M. Won, S.I. Park, Pathogenicity of *Vibrio harveyi* to cultured marine fishes in Korea, Aquaculture 285 (1–4) (2008) 8–13.
[13] S. Soto-Rodriguez, R. Lozano-Olvera, S. Abad-Rosales, J. Martínez-Brown, L. Ibarra-Castro, Susceptibility of Pacific white snook Centropomus viridis to Vibrio species, Dis. Aquat. Org. 134 (3) (2019) 189–195.
[14] A.M. Bjelland, A.K. Fauske, A. Nguyen, I.E. Orlien, I.M. Østgaard, H. Sørum, Expression of *Vibrio salmonicida* virulence genes and immune response parameters in experimentally challenged Atlantic salmon (*Salmo salar L.*), Front. Microbiol. 4 (2013) 401.
[15] S. Peeralil, T.C. Joseph, V. Murugadas, P. Akhilnath, V. Sreejith, K. Lalitha, *Vibrio harveyi* virulence gene expression in vitro and in vivo during infection in black tiger shrimp *Penaeus monodon*, Dis. Aquat. Org. 139 (2020) 153–160.
[16] S. Koshio, Immunotherapies targeting fish mucosal immunity-Current knowledge and future perspectives, Front. Immunol. 6 (2016) 643.
[17] J. Pérez-Sánchez, G. Terova, P. Simó-Mirabet, S. Rimoldi, O. Folkedal, J. A. Calduch-Giner, R.E. Olsen, A. Sitjà-Bobadilla, Skin mucus of gilthead sea bream (*Sparus aurata L.*). Protein mapping and regulation in chronically stressed fish, Front. Physiol. 8 (2017) 34.
[18] K.L. Shephard, Functions for fish mucus, Rev. Fish Biol. Fish. 4 (1994) 401–429.
[19] I. Salinas, The mucosal immune system of teleost fish, Biology 4 (3) (2015) 525–539.
[20] A. Giovanni, S. Maekawa, P.-C. Wang, S.C. Chen, Recombinant *Vibrio harveyi* flagellin A protein and partial deletions of middle variable region and D0 domain induce immune related genes in *Epinephelus coioides* and *Cyprinus carpio*, Dev. Comp. Immunol. 139 (2023) 104588.
[21] C.S.F. Raposo de Magalhães, M.A.C. Cerqueira, D. Schrama, M.J.V. Moreira, S. Boonanuntanasarn, P.M.L. Rodrigues, A Proteomics and other Omics approach in the context of farmed fish welfare and biomarker discovery, Rev. Aquacult. 12 (1) (2020) 122–144.
[22] B. Rajan, J. Lokesh, V. Kiron, M.F. Brinchmann, Differentially expressed proteins in the skin mucus of Atlantic cod (*Gadus morhua*) upon natural infection with *Vibrio anguillarum*, BMC Vet. Res. 9 (2013) 1–11.
[23] H.H. Liu, Q. Sun, Y.T. Jiang, M.H. Fan, J.X. Wang, Z. Liao, In-depth proteomic analysis of *Boleophthalmus pectinirostris* skin mucus, J. Proteonomics 200 (2019) 74–89.
[24] Y. Jiang, S. Zhou, W. Chu, The effects of dietary Bacillus cereus QSI-1 on skin mucus proteins profile and immune response in Crucian Carp (*Carassius auratus gibelio*), Fish Shellfish Immunol. 89 (2019) 319–325.
[25] Y. Xiong, C. Dan, F. Ren, Z. Su, Y. Zhang, J. Mei, Proteomic profiling of yellow catfish (*Pelteobagrus fulvidraco*) skin mucus identifies differentially-expressed proteins in response to *Edwardsiella ictaluri* infection, Fish Shellfish Immunol. 100 (2020) 98–108.
[26] Á. Fernández-Montero, S. Torrecillas, D. Montero, F. Acosta, M.J. Prieto-Álamo, N. Abril, J. Jurado, Proteomic profile and protease activity in the skin mucus of greater amberjack (*Seriola dumerili*) infected with the ectoparasite *Neobenedenia girellae*-An immunological approach, Fish Shellfish Immunol. 110 (2021) 100–115.
[27] N. Zhao, L. Jia, X. He, B. Zhang, Proteomics of mucosal exosomes of *Cynoglossus semilaevis* altered when infected by *Vibrio harveyi*, Dev. Comp. Immunol. 119 (2021) 104045.
[28] R. Hoare, K. Shahin, K. McLean, A. Adams, K.D. Thompson, Skin mucus proteins of rainbow trout (*Oncorhynchus mykiss*) in response to mucosal vaccination and challenge with *Flavobacterium psychrophilum*, J. Fish. Dis. 45 (3) (2022) 491.
[29] Y.Y. Li, J.X. Yang, X. Chen, Q. Chen, T.Y. Song, J.Q. Ge, Proteomic profiling skin mucus of European eel *Anguilla anguilla* infected with *Anguillid Herpesvirus*, Int. J. Mol. Sci. 23 (19) (2022) 11283.
[30] Y. Gu, W. Wang, Y. Zhan, X. Wei, Y. Shi, D. Cui, T. Peng, J. Han, X. Li, Y. Chen, Dietary artemisinin boosts intestinal immunity and healthy in fat greenling (*Hexagrammos otakii*), Front. Immunol. 14 (2023).
[31] M.A. Siddik, I.N. Vatsos, M.A. Rahman, H.D. Pham, Selenium-enriched spirulina (SeE-SP) enhance antioxidant response, immunity, and disease resistance in juvenile Asian seabass, Lates calcarifer, Antioxidants 11 (8) (2022) 1572.
[32] F.A. Guardiola, A. Cuesta, M. Arizcun, J. Meseguer, M.A. Esteban, Comparative skin mucus and serum humoral defence mechanisms in the teleost gilthead seabream (*Sparus aurata*), Fish Shellfish Immunol. 36 (2) (2014) 545–551.
[33] Y. Du, J. Gao, H. Zhang, X. Meng, D. Qiu, X. Gao, A. Zheng, Brain-targeting delivery of MMB4 DMS using carrier-free nanomedicine CRT-MMB4@ MDZ, Drug Deliv. 28 (1) (2021) 1822–1835.
[34] H. Zhang, T. Liu, Z. Zhang, S.H. Payne, B. Zhang, J.E. McDermott, J.Y. Zhou, V. A. Petyuk, L. Chen, D. Ray, Integrated proteogenomic characterization of human high-grade serous ovarian cancer, Cell 166 (3) (2016) 755–765.
[35] D. Zhang, Z. Yang, X. Song, F. Zhang, Y. Liu, TMT-based proteomic analysis of liquorice root in response to drought stress, BMC Genom. 23 (1) (2022) 524.
[36] C.H. Li, J. Chen, L. Nie, J. Chen, MOSPD2 is a receptor mediating the LEAP-2 effect on monocytes/macrophages in a teleost, *Boleophthalmus pectinirostris*, Zool. Res. 41 (6) (2020) 644–655.
[37] Y.Y. Yu, L.G. Ding, Z.Y. Huang, H.Y. Xu, Z. Xu, Commensal bacteria-immunity crosstalk shapes mucosal homeostasis in teleost fish, Rev. Aquacult. 13 (4) (2021) 2322–2343.
[38] J.B. Alexander, G.A. Ingram, Noncellular nonspecific defence mechanisms of fish, Annu. Rev. Fish Dis. 2 (1992) 249–279.
[39] M. Ángeles Esteban, An overview of the immunological defenses in fish skin, Int. Sch. Res. Notices (2012) 2012.
[40] L.B. Jensen, T. Wahli, C. McGurk, T.B. Eriksen, A. Obach, R. Waagbø, A. Handler, C. Tafalla, Effect of temperature and diet on wound healing in Atlantic salmon (*Salmo salar L.*), Fish Physiol. Biochem. 41 (2015) 1527–1543.
[41] M.D. Fast, Fish immune responses to parasitic copepod (namely sea lice) infection, Dev. Comp. Immunol. 43 (2) (2014) 300–312.
[42] G.J. Tserevelakis, M. Pavlidis, A. Samaras, G.D. Barmparis, K.G. Mavrakis, I. Draganidis, A. Oikonomou, E. Fanouraki, G.P. Tsironis, G. Zacharakis, Hybrid confocal fluorescence and photoacoustic microscopy for the label-free investigation of melanin accumulation in fish scales, Sci. Rep. 12 (1) (2022) 7173.
[43] U.W. Khan, Ø. Øverli, P.M. Hinkle, F.A. Pasha, I.B. Johansen, I. Berget, P.I. Silva, S. Kittilsen, E. Höglund, S.W. Omholt, A novel role for pigment genes in the stress response in rainbow trout (*Oncorhynchus mykiss*), Sci. Rep. 6 (1) (2016) 28969.
[44] S. Kittilsen, I.B. Johansen, B.O. Braastad, Ø. Øverli, Pigments, parasites and personality: towards a unifying role for steroid hormones? PLoS One 7 (4) (2012) e34281.
[45] M. Rajan, T. Banerjee, Histopathological changes induced by acute toxicity of mercuric chloride on the epidermis of freshwater catfish—*Heteropneustes fossilis* (Bloch), Ecotoxicol. Environ. Saf. 22 (2) (1991) 139–152.
[46] G.L. Wang, B.-H. Jiang, E.A. Rue, G.L. Semenza, Hypoxia-inducible factor 1 is a basic-helix-loop-helix-PAS heterodimer regulated by cellular O2 tension, Proc. Natl. Acad. Sci. USA 92 (12) (1995) 5510–5514.
[47] Z. Luo, M. Tian, G. Yang, Q. Tan, Y. Chen, G. Li, Q. Zhang, Y. Li, P. Wan, J. Wu, Hypoxia signaling in human health and diseases: implications and prospects for therapeutics, Signal Transduct. Targeted Ther. 7 (1) (2022) 218.
[48] B. Pei, K. Chen, S. Zhou, D. Min, W. Xiao, IL-38 restrains inflammatory response of collagen-induced arthritis in rats via SIRT1/HIF-1α signaling pathway, Biosci. Rep. 40 (5) (2020) BSR20182431.
[49] Y. Pan, Y. Yu, X. Wang, T. Zhang, Tumor-associated macrophages in tumor immunity, Front. Immunol. 11 (2020) 583084.
[50] L. Yang, D. Han, Z.-a. Wang, N. Chen, H. Zuo, Z. Guo, M. Xu, S. Weng, J. He, X. Xu, The Hippo-Yki Pathway Downstream Transcription Factor Scalloped Negatively Regulates Immune Defense against *Vibrio Parahaemolyticus* Infection in Shrimp, Fish & Shellfish Immunology, 2023 108917.
[51] Y. Cheng, J. Chen, Y. Shi, X. Fang, Z. Tang, MAPK signaling pathway in oral squamous cell carcinoma: biological function and targeted therapy, Cancers 14 (19) (2022) 4625.
[52] W. Zhang, H.T. Liu, MAPK signal pathways in the regulation of cell proliferation in mammalian cells, Cell Res. 12 (1) (2002) 9–18.
[53] N. Zhao, L. Jia, G. Li, X. He, C. Zhu, B. Zhang, Comparative mucous miRomics in *Cynoglossus semilaevis* related to *Vibrio harveyi* caused infection, Mar. Biotechnol. 23 (2021) 766–776.
[54] Y. Gao, Q. Shang, W. Li, W. Guo, A. Stojadinovic, C. Mannion, Y.G. Man, T. Chen, Antibiotics for cancer treatment: a double-edged sword, J. Cancer 11 (17) (2020) 5135.
[55] J. Dong, W. Wang, W. Zhou, S. Zhang, M. Li, N. Li, G. Pan, X. Zhang, J. Bai, C. Zhu, Immunomodulatory biomaterials for implant-associated infections: from conventional to advanced therapeutic strategies, Biomater. Res. 26 (1) (2022) 72.
[56] Z. Guo, W. Xu, G. Xu, Q. Jia, An updated overview of MOF@ MIP in drug carrier and drug analysis: construction, application and prospective, TrAC, Trends Anal. Chem. (2023) 117275.
[57] M. Dogterom, G.H. Koenderink, Actin–microtubule crosstalk in cell biology, Nat. Rev. Mol. Cell Biol. 20 (1) (2019) 38–54.
[58] Y. Huang, S. Zhang, J.-I. Park, Nuclear Actin Dynamics in Gene Expression, DNA Repair, and Cancer, Nuclear, Chromosomal, and Genomic Architecture in Biology and Medicine, Springer2022, pp. 625-663..
[59] F. Parker, T.G. Baboolal, M. Peckham, Actin mutations and their role in disease, Int. J. Mol. Sci. 21 (9) (2020) 3371.
[60] K. Niebuhr, S. Giuriato, T. Pedron, D.J. Philpott, F. Gaits, J. Sable, M.P. Sheetz, C. Parsot, P.J. Sansonetti, B. Payrastre, Conversion of PtdIns (4, 5) P2 into PtdIns (5) P by the S. flexneri effector IpgD reorganizes host cell morphology, EMBO J. 21 (19) (2002) 5069–5078.
[61] L. Chen, D.B. Flies, Molecular mechanisms of T cell co-stimulation and co-inhibition, Nat. Rev. Immunol. 13 (4) (2013) 227–242.
[62] S. Silvaraj, I.S.M. Yasin, M.M.A. Karim, M.Z. Saad, Transcriptome analysis of immune response in recombinant cell vaccine expressing OmpK vaccinated juvenile seabass (*lates calcarifer*) head kidney against vibrio harveyi infection, Aquaculture Reports 21 (2021) 100799.